

# First-principles atomistic Wulff constructions for gold nanoparticles

Georgios D. Barmparis

*Department of Materials Science and Technology,  
University of Crete, 71003 Heraklion, Crete, Greece and*

*Institute of Electronic Structure & Laser, Foundation for Research and Technology-Hellas, Heraklion, Crete, 71110, Greece\**

Ioannis N. Remediakis

*Department of Materials Science and Technology,  
University of Crete, 71003 Heraklion, Crete, Greece†*

(Dated: November 27, 2024)

We present a computational study for the equilibrium shape of gold nanoparticles. By linking extensive quantum-mechanical calculations, based on Density-Functional Theory (DFT) to Wulff construction, we predict equilibrium shapes that are in good agreement with experimental observations. We discuss the effect of the interactions between a nanoparticle and the encapsulating material on the equilibrium shape. As an example, we calculate adsorption of CO on several different Au(*hkl*) and use the results to explain the experimentally observed shape change of Au nanoparticles.

PACS numbers: 81.10.Aj, 82.65.+r, 68.43.Fg

Keywords: Gold; Density Functional calculations; Nanoparticles; Surface Science; Adsorption; Nanomaterials

Bulk gold is the noblest of all metals<sup>1</sup>, as demonstrated by delicate gold jewels manufactured several millennia ago which are found intact in excavations. On the other hand, catalysts that include oxide-supported gold nanoparticles were found to efficiently oxidize CO at room temperature<sup>2-4</sup>; Au is by far the best such catalyst<sup>5</sup>. Among the key factors that determine the efficiency of Au catalysts is the shape of Au nanoparticles, in particular the 5- and 6-fold coordinated atoms at its corners<sup>6-8</sup>.

The shape of Au nanoparticles has a key role in every aspect of their functionality, from sensing<sup>9</sup> and biolabeling applications<sup>10</sup> to plasmonics<sup>11</sup> and photonics<sup>12</sup>. In optoelectronics, quantum leaps between electronic states transform light into electricity and vice versa. The probability of such a transition depends on the density of states and the dipole matrix elements according to Fermi's golden rule. For a given size, both wavefunctions and energies depend critically on the nanoparticle shape. For example, the lowest excitation energy for a cubic nanoparticle is 10% higher than that of a spherical nanoparticle of the same volume<sup>13</sup>.

Gold nanoparticles are often found in their equilibrium shape. This is a polyhedron enclosed by faces of various (*hkl*) crystal orientations such that the total surface energy,

$$\sum_{hkl} A_{hkl} \gamma_{hkl}, \quad (1)$$

is minimum.  $A_{hkl}$  is the total area of faces parallel to (*hkl*) plane of the crystal and  $\gamma_{hkl}$  is the surface tension, i.e. the energy required to create a surface of unit area that is parallel to the (*hkl*) plane of the crystal. In order to predict equilibrium shape, one needs calculations of surface tensions for many different (*hkl*). Several such calculations exist in the literature either based on empirical potentials<sup>14</sup> or limited to Miller indexes of 0 and

1<sup>15</sup>, or using quantum-mechanics for low-index faces and empirical models for higher indexes<sup>16</sup>. An accurate and systematic calculation of all high-index Au surfaces is missing.

The equilibrium shape is often found to change upon exposure to some interacting environment. As Au nanoparticles are used in CO oxidation catalysis, CO gas is the ideal candidate to test this idea. Changes to shapes of higher sphericity upon exposure to CO gas have been observed both experimentally<sup>17</sup> and theoretically<sup>18</sup>. The interface tension of a metal in equilibrium with a gas is found to depend on the surface tension, the adsorption energy and the coverage of adsorbates Eq. (4). In order to predict the equilibrium shape in an interacting environment using the Wulff construction method, it is necessary to have a systematic calculation of adsorption energies for all relevant (*hkl*) surfaces.

The Wulff construction has been used to predict equilibrium shapes in a variety of systems. Wulff polyhedra are often employed in observations and models for nanomaterials including Cu catalysts<sup>19,20</sup>, or semiconductors<sup>21</sup>. In the past decade, Wulff shapes employing surface tensions from first-principles calculations were used for the successful prediction of the shape of nanoparticles, including interactions with their environment<sup>22-28</sup>. In the context of ammonia-synthesis catalysis, an *ab initio* determination of a nanoparticle shape was used as a first step in the creation of a virtual nano-catalyst<sup>29-31</sup>. In that work, the Wulff polyhedron was filled with atoms in order to create a realistic nanoparticle. The advantage of this method was that it allowed for detailed analysis of the atomic positions, making it possible to calculate structural quantities such as the number of active sites. This virtual nano-catalyst was used in other similar reactions, such as ammonia decomposition<sup>31</sup>. Here, we expand this methodology by including all possible (*hkl*) orientations. Moreover, we

take into account changes in shape that may be induced by interactions between the nanoparticle and its environment. We apply our method to supported gold nanoparticles, a system of high technological importance.

The paper is organised as follows: in Section I, we briefly review Wulff's theory regarding the equilibrium shape. In Section II, we present a systematic calculation of the surface tension for every Au( $hkl$ ) with Miller indexes up to 4. In section III, we use these surface tensions to create atomistic models for Au nanoparticles of sizes up to 70 nm, and analyse their structural properties, such as the concentration of active sites. In Section IV, we generalize our methodology for nanoparticles in interacting environment. We provide a simple formula that relates the interface tension to the surface tension and adsorption energy. We calculate the minimum adsorption energy of CO on every Au surface with Miller indexes up to 3, and use these results to calculate the change in equilibrium shape of Au particles upon exposure to CO gas. We summarize our results in Section V.

## I. THE WULFF CONSTRUCTION

The concept of "equilibrium shape" was postulated by Gibbs in the late 19th century. Under thermodynamic equilibrium, a given quantity of matter will attain a shape that minimizes the total surface energy of the system. More than a century ago, mineralogist G. Wulff proposed that the shape that minimizes Eq. (1) is such that the distance of each face from the center is proportional to the surface tension of the respective ( $hkl$ ) surface<sup>32</sup>:

$$d_{hkl} \sim \gamma_{hkl}. \quad (2)$$

One begins the Wulff construction by drawing up a plane (for example, (111)) at a distance  $d_{111}$  from the origin followed by planes parallel to ( $hkl$ ) at distances  $d_{hkl} = d_{111}\gamma_{hkl}/\gamma_{111}$ . The equilibrium shape will be the polyhedron enclosed by these planes, having thus the following properties:

- (a) The shape depends on ratios between surface tensions, and not their absolute values.
- (b) ( $hkl$ ) planes with high surface tension (usually high-indexed ones) will be drawn at greater distances and are therefore less likely to appear in the equilibrium shape.
- (c) Being steeper, high-index faces are usually hidden behind low-index ones, and tend to occupy smaller areas in the equilibrium shape even if  $\gamma_{hkl}$  is low.
- (d) The extra energy associated with the formation of edges between two surfaces is not taken into account.

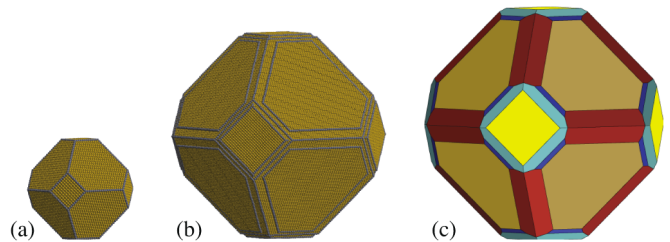


FIG. 1. (Color online) Typical calculated Au nanoparticles for various sizes,  $d$ : (a)  $d = 12.1$  nm (b)  $d = 27.2$  nm (c)  $d \rightarrow \infty$ . In (a) and (b), step and kink atoms are shown in darker color. In (c), different colors correspond to different kinds of surfaces. (c) was created using Wulffman<sup>33</sup>.

- (e) The Wulff polyhedron belongs to the same point group as the crystal structure of the material.

In addition to Wulff construction, there exist other methods for the study of nanoparticles. Advances in computers allow for the direct simulation of nanoparticles of large sizes using empirical potentials, as done for example by McKenna<sup>18</sup>. In that work, a large number of different shapes are tested to find the lowest-energy one. The Wulff construction is complimentary to that method. Here, we use Wulff construction coupled to first-principles calculations of surface tensions. This method offers a systematic, easy-to-follow recipe for the construction of atomistic models of nanoparticles.

## II. SURFACE TENSION OF GOLD SURFACES

As we are interested in relatively large Au nanoparticles, we limit our study to nanoparticles where Au atoms far from the surfaces are in the ideal fcc lattice. This is observed in simulations of large clusters<sup>34</sup>, although small gold clusters may have structures very different from fcc<sup>35</sup>. We begin by calculating the surface tension,  $\gamma_{hkl}$ , of Au by simulations of periodic ( $hkl$ ) slabs using Density-Functional Theory (DFT). We use the open-source Dacapo/ASE suite (<https://wiki.fysik.dtu.dk>). We use a plane wave basis with 340 eV cut-off. The core electrons are treated with Vanderbilt non-local ultrasoft pseudopotentials<sup>36</sup>. The Brillouin zone of the (111)-(1 $\times$ 1) surface is modelled by a (10 $\times$ 10 $\times$ 1) Monkhorst-Pack grid of  $\vec{k}$ -points; number of  $\vec{k}$ -points in other surfaces is calculated in proportionality to the (111) cell. We use the generalized gradient approximation (GGA) Perdew-Wang exchange-correlation functional PW91 for the clean surfaces and the revised Perdew-Burke-Ernzerhof functional RPBE for the surfaces covered with CO since this one gives better adsorption energies<sup>37</sup>. For each set of calculations, we use the theoretical lattice constant which is found to be 4.22 Å for RPBE and 4.18 Å for PW91, very close to the experimental value of 4.08 Å. There is a general trend to slightly overestimate the lattice constant of noble metals

	This work	calc <sup>14</sup>	calc <sup>16</sup>	calc <sup>15</sup>	$E_{ads}$ (eV)
$\gamma_{100}/\gamma_{111}$	1.23	1.11	1.15	1.27	-0.25 (b)
$\gamma_{110}/\gamma_{111}$	1.29	1.24	1.22	1.33	-0.36 (b)
$\gamma_{210}/\gamma_{111}$	1.33	1.31	1.29		-0.49 (t)
$\gamma_{211}/\gamma_{111}$	1.17	1.19	1.18		-0.34 (t)
$\gamma_{221}/\gamma_{111}$	1.14	1.16	1.15		-0.35 (t)
$\gamma_{310}/\gamma_{111}$	1.31	1.28	1.28		-0.51 (t)
$\gamma_{311}/\gamma_{111}$	1.26	1.24	1.22		-0.32 (b)
$\gamma_{320}/\gamma_{111}$	1.36	1.30	1.28		-0.48 (t)
$\gamma_{321}/\gamma_{111}$	1.25	1.26	1.23		-0.50 (t)
$\gamma_{322}/\gamma_{111}$	1.11	1.13	1.12		-0.34 (t)
$\gamma_{331}/\gamma_{111}$	1.18	1.21	1.19		-0.34 (t)
$\gamma_{332}/\gamma_{111}$	1.07	1.11	1.11		-0.35 (t)
$\gamma_{410}/\gamma_{111}$	1.32	1.25	1.26		-0.49 <sup>f</sup>
$\gamma_{411}/\gamma_{111}$	1.27	1.23	1.22		-0.34 <sup>f</sup>
$\gamma_{421}/\gamma_{111}$	1.32	1.29	1.26		-0.49 <sup>f</sup>
$\gamma_{430}/\gamma_{111}$	1.34	1.29	1.27		-0.49 <sup>f</sup>
$\gamma_{431}/\gamma_{111}$	1.27	1.27	1.25		-0.49 <sup>f</sup>
$\gamma_{432}/\gamma_{111}$	1.19	1.20	1.18		-0.49 <sup>f</sup>
$\gamma_{433}/\gamma_{111}$	1.09	1.09	1.09		-0.34 <sup>f</sup>
$\gamma_{441}/\gamma_{111}$	1.22	1.22	1.21		-0.34 <sup>f</sup>
$\gamma_{443}/\gamma_{111}$	1.06	1.09	1.08		-0.34 <sup>f</sup>

TABLE I. Ratios of surface tensions of Au in comparison to other calculations. The last column contains the adsorption energy of CO at low coverage on the same ( $hkl$ ) surface, and the adsorption geometry. b=bridge adsorption, t=on-top adsorption. <sup>f</sup>: energies calculated from the linear fit shown in Fig. 2.

using GGA<sup>38</sup>. We model all ( $hkl$ ) surfaces of fcc Au with indexes up to 4. Even for CO-covered nanoparticles, no ( $4kl$ ) surfaces are observed in the Wulff construction; for this reason we do not consider ( $5kl$ ) surfaces in this work. Atoms in the top two layers from each side are allowed to relax, while subsequent slabs are separated by 12 Å of vacuum. Slab thickness is chosen independently for each ( $hkl$ ) slab until the surface tension converges within 0.01 J/m<sup>2</sup>. The surface tension,  $\gamma_{hkl}$  is derived from

$$E_{slab} = NE_{bulk} + 2A\gamma_{hkl}, \quad (3)$$

where  $N$  is the number of atoms in the slab,  $E_{slab}$  is the total energy of the slab,  $E_{bulk}$  is the energy per atom in bulk Au and  $A$  is the area parallel to ( $hkl$ ).

The results are summarized in Table I. Interestingly, the ratio of surface energies of different cells is very close to the ratio of the areal density of cleaved bonds<sup>16</sup>. This is another example of the unique chemistry of Au<sup>1</sup>: Au atoms have a closed  $d$ -shell and have the least preference for directional bonds in the entire periodic table. The calculated absolute value for  $\gamma_{111}$  is 0.69 J/m<sup>2</sup>, very close to 0.64 J/m<sup>2</sup> reported by Wen and Zhang<sup>14</sup> and within the same order of magnitude as the values reported by state-of-the-art relativistic all-electron calculations<sup>15,16</sup>. The nanoparticle shape depends only on ratios between surface energies. As shown in Table I, our results for the ratios between surface tensions agree with more detailed calculations within 5% or less.

### III. AU NANOPARTICLES IN NON-INTERACTING ENVIRONMENT

The Wulff construction for Au is shown in Fig. 1(c). It contains 144 vertices and 86 faces of 5 different kinds: (111), (100), (332), (211) and (322) in order of total area.

To construct atomistic models for nanoparticles, we start from a large fcc crystal. As (111) has the lowest surface tension, we begin by choosing the number of (111) layers. This determines the distance of (111) plane from the center of the nanoparticle,  $d_{111}$ , and, consequently, the nanoparticle size. For other faces, we use Eq. (2), with the calculated values of  $\gamma_{hkl}$  and cut the crystal at the correct distances  $d_{hkl}$ . We calculate the equation of the plane defined by every set of three surface atoms, and make sure that only faces consistent with the Wulff construction appear on the nanoparticle. We consider about 30000 different nanoparticles with diameters ranging from 1.7 nm to more than 100 nm.

At small sizes, some faces might not be large enough to accommodate a single atom, let alone a unit cell of this. Very small nanoparticles expose only (111) and (100) faces; in particular, our simulated 459-atom nanoparticle is identical to the one found from simulations and X-ray experiments<sup>34</sup>. In all cases, the shape resembles a truncated octahedron consisting mainly of (111) and (100) faces, with their edges decorated by several ( $hkl$ ) faces with indexes up to 3. For diameters up to 16.3 nm, we find only (111) and (100) faces; as the nanoparticle grows in size, different ( $hkl$ ) orientations start to appear. The thermodynamic limit, shown in 1(c) is reached at diameters of the order of 100 nm.

Geometrical features or typical nanoparticles are shown in Table II. The area of nanoparticles is calculated analytically using the coordinates of vertices; their volume is obtained by numerical integration. By fitting over a hundred particles of different diameters, we provide scaling relations of various properties with total number of atoms, in accordance with atom-counting models for nanoparticles<sup>39,40</sup>.

### IV. AU NANOPARTICLES IN INTERACTING ENVIRONMENT

The equilibrium shape of nanoparticles that interact with their environment can be found by means of a Wulff construction based on interfacial tensions,  $\gamma_{hkl}^{int}$ , between Au and its environment instead of surface tensions,  $\gamma_{hkl}$ . It turns out that the two are related by a simple formula:

$$\gamma_{hkl}^{int} = \gamma_{hkl} + \theta \frac{E_{ads}}{A_{at}}, \quad (4)$$

where  $\theta$  is the coverage (number of metal-adsorbate bonds over number of surface atoms),  $A_{at}$  is total surface area per metal atom and  $E_{ads}$  the adsorption energy, defined as the excess energy per molecule of the system

Shape	d (nm)	$N_{corner}$	$N_{edge}$	$N_{surf}$	$N_{tot}$	Area (nm <sup>2</sup> )	Volume (nm <sup>3</sup> )	Faces
(a)	12.12	24	444	5208	42925	438	730	(111), (100) (86%), (14%)
(b)	27.17	96	2832	25998	473550	2275	8439	(111), (332), (211), (100) (58%), (16%), (15%), (11%)
(c)	$0.31N^{0.34}$	144	$6N^{0.40}$	$3N^{0.68}$	N	$0.3N^{0.67}$	0.02N	(111),(332),(211),(100),(322)

TABLE II. Characteristic data for typical nanoparticles shown in Fig. 1. Shape (a) is typical for particles up to  $d = 16.3$  nm in diameter, shape (b) is typical for larger particles and (c) presents fitted values from over a hundred different particles with  $d < 16.3$  Å.  $N_{corner}$ ,  $N_{edge}$  and  $N_{surf}$  are the total number of atoms at vertices, edges and faces of the nanoparticle, respectively;  $N_{total}$  is the total number of atoms.  $A$  is the total surface area and  $V$  the volume of the nanoparticle.  $(hkl)$  are the appearing surfaces in the shape with the percentage of the total area they occupy.

compared to isolated Au surface and isolated encapsulating material. Eq. (4) includes implicitly the effects of adsorbate-adsorbate interactions, as both the adsorption energy and the equilibrium coverage depend on such interactions.

To prove Eq.(4), we use the definitions of  $\gamma^{int}$  and  $E_{ads}$  for a slab of metal in equilibrium with some material X:

$$E_{slab+X} = NE_{bulk} + N_{ads}E_X + 2A\gamma_{hkl}^{int}, \quad (5)$$

$$E_{slab+X} = E_{slab} + N_{ads}E_X + N_{ads}E_{ads}. \quad (6)$$

In the above equations,  $E_{slab+X}$  is the total energy of the slab+X system,  $E_X$  is the total energy per molecule of X, and  $N_{ads}$  is the number of bonds between slab and X. The latter is related to the coverage,  $\theta$  and area per surface atom,  $A_{at}$ , by  $\theta = N_{ads}/N_{surf}$  and  $A = A_{at}N_{surf}$ . Substituting into Eqs. (5) and (6) and using Eq. (3) yields Eq. (4).

For a typical system ( $\theta = 0.1$ ,  $E_{ads}=0.5$  eV), the second term in Eq.(4) is about 0.1 J/m<sup>2</sup>, or 10% of  $\gamma_{hkl}$ . Change in ratios between various  $\gamma_{hkl}$  will be of the order of 1%, resulting in very small change in the equilibrium shape. This explains the similarity of nanoparticle shapes observed in a wide variety of environments: our simulations nicely match experimental observations, not only for Au clusters<sup>34</sup> but also Au particles on C nanotubes<sup>41,42</sup>, on TiO<sub>2</sub><sup>43</sup> and on CeO<sub>2</sub><sup>4</sup>.

On the other hand, shape can change dramatically for very small nanoparticles where bonding on faces might be very different from bonding on a large surface<sup>44,45</sup> or when small molecules with high adsorption energy are adsorbed. The ideal adsorbate to test this idea is CO.

We calculate the minimum adsorption energy of CO on every Au( $hkl$ ) with  $h, k, l \leq 3$ . We consider several different adsorption sites to ensure that the global minimum is found; as we are interested in very low CO coverage, neighbouring CO molecules maintain a distance of more than 4.2 Å at all cases. In almost every case, CO binds atop the lowest-coordinated Au atom with adsorption energy being a linear function of the coordination number of this Au atom,  $z$  (Fig. 2)<sup>6-8,46</sup>. We use this linear fit to obtain adsorption energies for the nine ( $4kl$ ) surfaces.

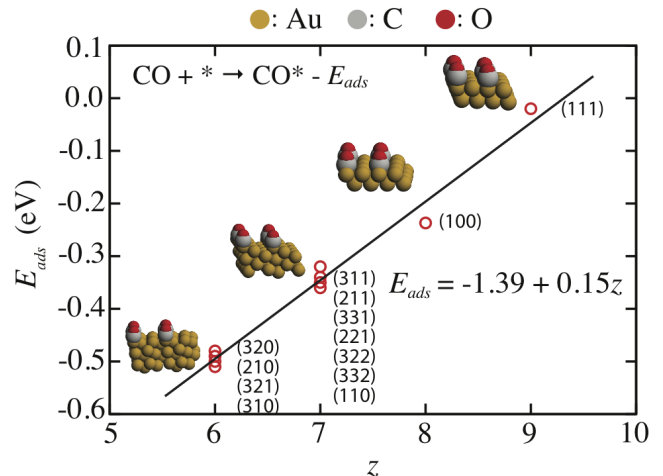


FIG. 2. (Color online) Adsorption energy of CO on Au( $hkl$ ) as a function of the Au coordination number,  $z$ , and its linear fit. Some characteristic adsorption geometries are shown.

Adsorption energies and adsorption sites are shown in Table I.

We use calculated adsorption energies together with Eq. (4) and obtain the equilibrium shape of Au nanoparticles at low CO coverage shown in Fig. 3. For rough surfaces,  $\gamma_{hkl}$  will be relatively high, but at the same time  $E_{ads}$  will be quite low; this results in a compensation effect for the two terms in Eq. (4). As the different  $\gamma_{hkl}^{int}$  are close to each other, the shape has a much higher sphericity<sup>47</sup> (98%) than the shape in vacuum (93%), in excellent agreement with experiments<sup>4,17</sup>.

Exposure of the nanoparticle to CO gas makes it much more reactive. This effect has been observed in first-principles simulations of small Au clusters<sup>7,18,48</sup>. We find that the same happens at larger sizes, although it is more prominent for smaller nanoparticles. Assuming that all step-edge atoms are active, the active-site density doubles, increasing from about 200  $\mu\text{mol/g}$  to 400  $\mu\text{mol/g}$  for the nanoparticle shown in Fig. 3.

Gold nanoparticles are usually supported on oxides, such as MgO or rutile TiO<sub>2</sub>. The interaction between the nanoparticle and the supporting material will also affect

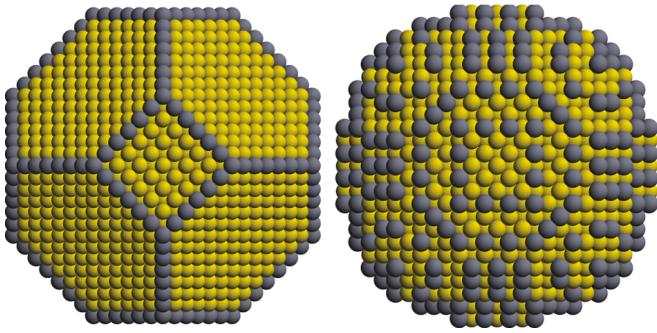


FIG. 3. (Color online) Left: Model of a typical Au nanoparticle ( $d = 5.4$  nm, ca. 5000 atoms) in weakly interacting environment (sphericity=93%, 200  $\mu\text{mol}$  of active sites per g) Right: a same size nanoparticle in equilibrium with low-pressure CO gas (sphericity=98%, 400  $\mu\text{mol}$  of active sites per g). Step and kink atoms are shown in darker color.

its shape. The epitaxial growth will introduce strain in the nanoparticle<sup>21</sup>. More important, the values of  $\gamma_{hkl}$  for the faces attached to the supporting material will be very different. A qualitative picture of this interaction has been presented by Lopez *et al.*<sup>49</sup>.

## V. SUMMARY

We have developed a method for constructing and characterizing equilibrium-shaped nanoparticles in ther-

modynamic equilibrium with their environment. Using an atomistic version of the Wulff construction, we generate Cartesian positions of nanoparticles, which can then be used to analyse structural properties. Our results provide insight into large nanoparticles that are of interest to catalysis, but are inaccessible by direct atomistic simulations. The calculated nanoparticles match experimental results, including the similarity of shapes in weakly interacting systems as well as the change towards more spherical shapes upon exposure to reactive gas. The method is easily generalized to other materials, and might be useful for the improved design of nanomaterials with tailored physical and chemical properties.

## ACKNOWLEDGMENTS

This work was supported by COST action MPMP0901 (NanoTP) and by the Research Council, University of Crete. The authors acknowledge support and inspiring discussions with Prof. S. Farantos.

\* Electronic Address: barmparis@materials.uoc.gr

† Electronic Address: remed@materials.uoc.gr; Group Web Page: <http://theory.materials.uoc.gr>

<sup>1</sup> B. Hammer and J. K. Nørskov, *Nature* **376**, 238 (1995).

<sup>2</sup> M. Haruta, N. Yamada, T. Kobayashi, and S. Iijima, *J. Catal.* **115**, 301 (1989).

<sup>3</sup> M. Valden, X. Lai, and D. W. Goodman, *Science* **281**, 1647 (1998).

<sup>4</sup> T. Uchiyama, H. Yoshida, Y. Kuwauchi, S. Ichikawa, S. Shimada, M. Haruta, and S. Takeda, *Angew. Chem. Int. Edit.* **50**, 10157 (2011).

<sup>5</sup> H. Falsig, B. Hvolbaek, I. S. Kristensen, T. Jiang, T. Bligaard, C. H. Christensen, and J. K. Nørskov, *Angew. Chem. Int. Ed.* **47**, 4835 (2008).

<sup>6</sup> N. Lopez and J. K. Nørskov, *J. Am. Chem. Soc.* **124**, 11262 (2002).

<sup>7</sup> I. N. Remediakis, N. Lopez, and J. K. Nørskov, *Angew. Chem. Int. Edit.* **44**, 1824 (2005).

<sup>8</sup> I. N. Remediakis, N. Lopez, and J. K. Nørskov, *Appl. Catal. A-Gen.* **291**, 13 (2005).

<sup>9</sup> Y. Kim, R. Johnson, and J. Hupp, *Nano Lett.* **1**, 165 (2001).

<sup>10</sup> E. Boisselier and D. Astruc, *Chem. Soc. Rev.* **38**, 1759 (2009).

<sup>11</sup> S. Lal, S. Link, and N. J. Halas, *Nat. Photonics* **1**, 641 (2007).

<sup>12</sup> Y. Lu, Y. Yin, Z. Li, and Y. Xia, *Nano Lett.* **2**, 785 (2002).

<sup>13</sup> For cube of edge  $a$ ,  $\Delta E = \frac{\hbar^2 \pi^2}{2ma^2}$ ; for a sphere of radius  $r$ ,  $\Delta E = \frac{\hbar^2 (\chi_{11} - \chi_{10})}{2mr^2}$ , where  $\chi_{11}, \chi_{10}$  are the first two roots of the spherical Bessel function  $j_1(x)$ .

<sup>14</sup> Y.-N. Wen and J.-M. Zhang, *Solid State Commun.* **144**, 163 (2007).

<sup>15</sup> L. Vitos, A. V. Ruban, H. L. Skriver, and J. Kollr, *Surf. Sci.* **411**, 186 (1998).

<sup>16</sup> I. Galanakis, G. Bihlmayer, V. Bellini, N. Papanikolaou, R. Zeller, S. Blügel, and P. H. Dederichs, *Europhys. Lett.* **58**, 751 (2002).

<sup>17</sup> K. Ueda, T. Kawasaki, H. Hasegawa, T. Tanji, and M. Ichihashi, *Surf. Interface Anal.* **40**, 1725 (2008).

<sup>18</sup> K. P. McKenna, *Phys. Chem. Chem. Phys.* **11**, 4145 (2009).

<sup>19</sup> B. S. Clausen, J. Schiøtz, L. Gråbæk, C. V. Ovesen, K. W. Jacobsen, J. K. Nørskov, and H. Topsøe, *Top. Catal.* **1**, 367 (1994).

<sup>20</sup> P. L. Hansen, J. B. Wagner, S. Helveg, J. R. Rostrup-Nielsen, B. S. C. BS, and H. Topsøe, *Science* **295**, 2053 (2002).

<sup>21</sup> P. Müller and R. Kern, *Surf. Sci.* **457**, 229 (2000).

<sup>22</sup> A. Barnard and P. Zapol, *J. Chem. Phys.* **121**, 4276 (2004).

<sup>23</sup> A. S. Barnard and L. A. Curtiss, *Nano Lett.* **5**, 1261 (2005).

<sup>24</sup> G. Hadjisavvas, I. N. Remediakis, and P. C. Kelires, *Phys. Rev. B* **74**, 165419 (2006).

- <sup>25</sup> G. Kopidakis, I. N. Remediakis, M. G. Fyta, and P. C. Kelires, *Diam. Relat. Mater.* **16**, 1875 (2007).
- <sup>26</sup> F. Mittendorfer, N. Seriani, O. Dubay, and G. Kresse, *Phys. Rev. B* **76**, 233413 (2007).
- <sup>27</sup> A. Soon, L. Wong, B. Delley, and C. Stampfl, *Phys. Rev. B* **77**, 125423 (2008).
- <sup>28</sup> H. Shi and C. Stampfl, *Phys. Rev. B* **77**, 094127 (2008).
- <sup>29</sup> K. Honkala, A. Hellman, I. N. Remediakis, A. Logadottir, A. Carlsson, S. Dahl, C. Christensen, and J. K. Nørskov, *Science* **307**, 558 (2005).
- <sup>30</sup> A. Hellman, K. Honkala, I. N. Remediakis, A. Logadottir, A. Carlsson, S. Dahl, C. H. Christensen, and J. K. Nørskov, *Surf. Sci.* **600**, 4264 (2006).
- <sup>31</sup> A. Hellman, K. Honkala, I. N. Remediakis, A. Logadottir, A. Carlsson, S. Dahl, C. H. Christensen, and J. K. Nørskov, *Surf. Sci.* **603**, 1731 (2009).
- <sup>32</sup> C. Herring, *Phys. Rev.* **82**, 87 (1951).
- <sup>33</sup> A. R. Roosen, R. P. McCormack, and W. C. Carter, *Comp. Mater. Sci.* **11**, 16 (1998).
- <sup>34</sup> C. L. Cleveland, U. Landman, M. N. Shafiqullin, P. W. Stephens, and R. L. Whetten, *Zeit. Phys. D* **40**, 503 (1997).
- <sup>35</sup> F. Baletto and R. Ferrando, *Rev. Mod. Phys.* **77**, 371 (2005).
- <sup>36</sup> D. Vanderbilt, *Phys. Rev. B* **41**, 7892 (1990).
- <sup>37</sup> B. Hammer, L. B. Hansen, and J. K. Nørskov, *Phys. Rev. B* **59**, 7413 (1999).
- <sup>38</sup> M. Fuchs, M. Bockstedte, E. Pehlke, and M. Scheffler, *Phys. Rev. B* **57**, 2134 (1998).
- <sup>39</sup> N. Lopez, T. Janssens, B. Clausen, Y. Xu, M. Mavrikakis, T. Bligaard, and J. K. Nørskov, *J. Catal.* **223**, 232 (2004).
- <sup>40</sup> N. V. Galanis, I. N. Remediakis, and G. Kopidakis, *Phys. Status Solidi C* **7**, 1372 (2010).
- <sup>41</sup> C. Bittencourt, A. Felten, B. Douhard, J.-F. Colomer, G. V. Tendeloo, W. Drube, J. Ghijsen, and J.-J. Pireaux, *Surf. Sci.* **601**, 2800 (2007).
- <sup>42</sup> M. Quintana, X. Ke, G. V. Tendeloo, M. Meneghetti, C. Bittencourt, and M. Prato, *ACS Nano* **4**, 6105 (2010).
- <sup>43</sup> S. Sivaramakrishnan, J. Wen, M. E. Scarpelli, B. J. Pierce, and J.-M. Zuo, *Phys. Rev. B* **82**, 195421 (2010).
- <sup>44</sup> M. Walter, J. Akola, O. Lopez-Acevedo, P. D. Jadzinsky, G. Calero, C. J. Ackerson, R. L. Whetten, H. Groenbeck, and H. Häkkinen, *P. Natl. Acad. Sci. USA* **105**, 9157 (2008).
- <sup>45</sup> W. D. Luedtke and U. Landman, *J. Phys. Chem. B* **102**, 6566 (1998).
- <sup>46</sup> G. Mpourmpakis, A. N. Andriotis, and D. G. Vlachos, *Nano Lett.* **10**, 1041 (2010).
- <sup>47</sup> Sphericity equals  $\pi^{1/3}(6V)^{2/3}/A$  where  $V$  is the volume and  $A$  the area of the nanoparticle; characteristic values are 81% for a cube, 85% for an octahedron and 100% for a sphere.
- <sup>48</sup> K. P. McKenna and A. L. Shluger, *J. Phys. Chem. C* **111**, 18848 (2007).
- <sup>49</sup> N. Lopez, J. Nørskov, T. Janssens, A. Carlsson, A. Puig-Molina, B. Clausen, and J.-D. Grunwaldt, *J. Catal.* **225**, 86 (2004).